

## Estimating Discrete Power Angular Spectra in Multiprobe OTA Setups

Fan, Wei; Nielsen, Jesper Ødum; Pedersen, Gert Frølund

*Published in:*

I E E E Antennas and Wireless Propagation Letters

*DOI (link to publication from Publisher):*

[10.1109/LAWP.2014.2306205](https://doi.org/10.1109/LAWP.2014.2306205)

*Publication date:*

2014

*Document Version*

Early version, also known as pre-print

[Link to publication from Aalborg University](#)

*Citation for published version (APA):*

Fan, W., Nielsen, J. Ø., & Pedersen, G. F. (2014). Estimating Discrete Power Angular Spectra in Multiprobe OTA Setups. *I E E E Antennas and Wireless Propagation Letters*, 13, 349 - 352.  
<https://doi.org/10.1109/LAWP.2014.2306205>

### General rights

Copyright and moral rights for the publications made accessible in the public portal are retained by the authors and/or other copyright owners and it is a condition of accessing publications that users recognise and abide by the legal requirements associated with these rights.

- Users may download and print one copy of any publication from the public portal for the purpose of private study or research.
- You may not further distribute the material or use it for any profit-making activity or commercial gain
- You may freely distribute the URL identifying the publication in the public portal -

### Take down policy

If you believe that this document breaches copyright please contact us at [vbn@aub.aau.dk](mailto:vbn@aub.aau.dk) providing details, and we will remove access to the work immediately and investigate your claim.

# Estimating Discrete Power Angular Spectra in Multi-probe OTA Setups

Wei Fan, Jesper Ø. Nielsen, and Gert F. Pedersen

**Abstract**—The paper discusses over the air (OTA) testing for multiple input multiple output (MIMO) capable terminals with emphasis on estimating discrete power angular spectrum modeled at the receiver (Rx) side in the test zone. Two techniques based on a uniform circular array (UCA) are proposed to obtain accurate direction of arrival estimates as well as power estimates of the impinging signals in the test zone. Simulation results match well with the target, as expected. Measurement results based on a virtual UCA in a practical 3D multi-probe setup further support the simulation results. Possible reasons for the deviations between simulations and measurements are also investigated.

**Index Terms**—MIMO OTA testing, multi-probe, anechoic chamber, power angular spectrum, antenna array

## I. INTRODUCTION

Field tests can fully evaluate mobile devices in a realistic environment. However, they may not be practical due to the high cost and lack of reproducibility of the results. Over the air testing (OTA) in the lab is an alternative to test device performance realistically. The multi-probe anechoic chamber method, due to its capability to physically approximate the realistic multipath environments in a shielded anechoic chamber, has been a promising candidate in standardizations to test multiple-input multiple-output (MIMO) capable terminals [1].

To evaluate the devices equipped with multiple antennas, it is critical to reproduce a specific propagation environment around the device under test (DUT). A continuous power angular spectrum (PAS) is often specified for a channel model at the receiver (Rx) side, see e.g. [2]. It is desirable that with a limited number of probes we should approximate the target continuous PAS. The spatial correlation, which is a statistical measure of the similarity between received signals at different receive (Rx) antennas, has been used to represent the channel spatial characteristics at the Rx side [3], [4]. The spatial correlation is used to determine the test zone size [4].

However, the PAS itself is interesting, not just through its effect on the Rx antenna (i.e. the spatial correlation at the Rx). The PAS of the channel at the Rx side modeled with the multiple probes is discrete, characterized by the angular locations and power weights of the active probes. The discrete PAS directly represent the directivity of the created channels and is preferable to the spatial correlation for certain channel models, e.g. the Rician fading channel models and the constant non-fading channel models. As demonstrated in [6], once the discrete PAS and DUT radiation patterns are known, other

interesting parameters, e.g. the spatial correlation accuracy for realistic DUTs, the test zone size, and the reproduced spatial correlation can be easily obtained. In practical multi-probe setups, knowledge on how the channel is emulated in commercial channel emulators is very limited. Estimation of the discrete PAS can be used to verify how well the target channel is implemented in the test area. Furthermore, spatial correlation measurements, which are proposed in [1] to verify the implemented channels would fail for 3D multi-probe setups, as an isotropic antenna does not exist in practice.

Unlike previous work that merely rely on the spatial correlation to model and estimate the channel spatial characteristics created at the Rx side, this paper intends to estimate the discrete PAS using the antenna array theory. While DoA estimation using antenna arrays have been well studied in the literature, the discrete PAS estimation in multi-probe based anechoic chamber setup has not been reported in the literature. The main contributions of this paper lie in three aspects:

- A technique based on a virtual uniform circular array (UCA) to estimate discrete PAS modeled in multi-probe setups is proposed. Simulation results show that the estimated discrete PAS matches well with the target.
- Measurement results based on a virtual UCA in a preliminary 3D multi-probe setup show that the techniques are useful in practice. Previous measurement results were mainly based on 2D multi-probe setups. However, elevation spread can not be ignored in many propagation environments, as demonstrated by measurements. Note that a more complicated practical 3D setup with more probes might be required to have the full flexibility to model arbitrary realistic 3D channel channels [7].
- Possible reasons that introduce deviation between the measurement and simulation results are given.

## II. METHODS

### A. Prefaded signal synthesis technique

The prefaded signal synthesis (PFS) method is a technique proposed for channel emulation in multi-probe based anechoic chamber setups in [4] and it has been implemented in several commercial channel emulators. The basic idea is to transmit Rayleigh or other kinds of fading signals separately from the multiple probes. A cluster is mapped to the multi-probes based on the cluster PAS and probe angular locations. An example is illustrated in Figure 1, where eight power weights for a single Laplacian shaped cluster is shown. Each probe associated with the cluster transmits weighted independent fading sequences with identical statistics. Contributions on obtaining optimal

Wei Fan, Jesper Ø. Nielsen, and Gert F. Pedersen are with the Antennas, Propagation and Radio Networking section at the Department of Electronic Systems, Faculty of Engineering and Science, Aalborg University, Denmark (email: {wfa, jni, gfp}@es.aau.dk).

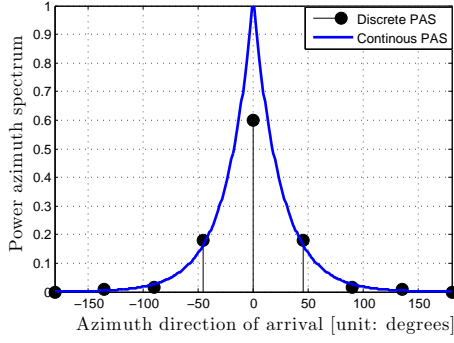


Figure 1. An illustration of the continuous and discrete PAS of a Laplacian shaped cluster with azimuth DoA  $0^\circ$  and azimuth angle spread  $35^\circ$ . The discrete angles define the angular locations of the probes.

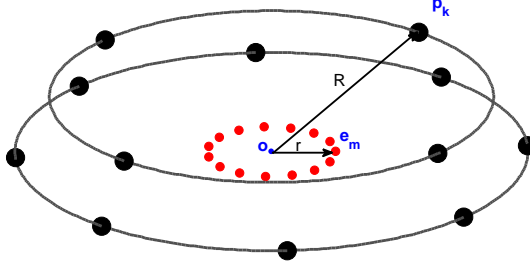


Figure 2. An illustration of the multi-probe setups and the antenna elements on the UCA. The number of probes is  $K$  and the number of array elements is  $M$ . The radius of the probe sphere  $R$  is assumed much larger than the radius of the UCA  $r$ .

power weights haven been discussed in [3], [4] and results from [3] are used in Figure 1.

In a practical multi-probe setup, the discrete PAS is generally unknown, as information on the commercial channel emulators is often very limited, and practical setup issues may effectively change the PAS. This paper intends to estimate the discrete PAS modeled in the multi-probe setups using a virtual UCA. The discrete PAS can be used to verify how well the channels are implemented in the lab. For the sake of simplicity, discrete PAS estimation of a single cluster is addressed in this paper. That is, the signals transmitted from the probes are narrowband. This can be easily extended to multiple cluster cases (i.e. wideband channels). Wideband measurements can be performed to detect the multiple delays in the wideband channels and the techniques proposed in the paper can be used to estimate the discrete PAS for each delay.

## B. Simulation model

1) *Problem formulation:* Figure 2 illustrates a multi-probe setup, where  $\vec{op_k}$  is a vector containing the angular location for the  $k$ th probe with  $k \in [1, K]$ . A UCA is used to estimate the discrete PAS, as probes are often placed around the DUT. Uniform linear arrays (ULAs) are not applicable, as two probes at locations symmetric with respect to the line can not be distinguished.  $\vec{oe_m}$  is a vector containing the angular location for the  $m$ th UCA element with  $m \in [1, M]$ .

The baseband model for the received signals at the array elements can be written in a matrix form as follows:

$$\mathbf{x}[n] = \mathbf{A}\mathbf{s}[n] + \mathbf{v}[n] \quad (1)$$

where:

- $\mathbf{x}[n] = \{x_m[n]\} \in \mathbb{C}^{M \times 1}$  is a vector containing  $M$  received signals at the  $n$ th snapshot.
- $\mathbf{A} = \{a_{mk}\} \in \mathbb{C}^{M \times K}$  is a transfer matrix of coefficients from the  $k$ th probe to the  $m$ th antenna element with

$$a_{mk} = c_{mk} \exp \left[ j \frac{2\pi}{\lambda} \frac{\vec{op_k} \cdot \vec{oe_m}}{|\vec{op_k}|} \right] \quad (2)$$

where  $(\cdot)$  is the dot operator and  $||$  is the norm operator.  $c_{mk}$  is the path loss term from the  $k$ th probes to the  $m$ th antenna element and it is a constant, as  $R \gg r$  is assumed.  $\lambda$  is the wavelength.

- $\mathbf{s}[n] = \{s_k[n]\} \in \mathbb{C}^{K \times 1}$  is a vector containing  $K$  transmitted signals at the  $n$ th snapshot.
- $\mathbf{v}[n] = \{v_m[n]\} \in \mathbb{C}^{M \times 1}$  is noise vector. As the study is performed in an anechoic chamber, the noise term is assumed small and neglected.

The auto-covariance matrix  $\hat{\mathbf{R}} \in \mathbb{C}^{M \times M}$  of the received signals can be estimated as:

$$\hat{\mathbf{R}} = \frac{1}{N} \sum_{n=1}^N \mathbf{x}[n] \mathbf{x}^H[n] \quad (3)$$

The power weights allocated to the probes depend on the target continuous PAS and probe angular locations, and hence some probes may not be used in synthesizing the channel.

2) *DoA estimation:* DoA estimation using antenna arrays has long been of research interest given their importance in a great variety of applications and various methods have been proposed [8]. As explained in Sec. II-A, transmit signals from the multiple probes are uncorrelated and narrowband. Two basic DoA estimation algorithms are discussed below.

The  $m$ th component of the steering vector  $\mathbf{a}(\theta, \varphi) = \{a_m(\theta, \varphi)\} \in \mathbb{C}^{M \times 1}$  for a UCA can be expressed as:

$$a_m(\theta, \varphi) = \exp \left[ j \frac{2\pi}{\lambda} r \sin \theta \cos(\varphi - \gamma_m) \right] \quad (4)$$

where  $\theta$  and  $\varphi$  are the elevation and azimuth angle, respectively.  $\gamma_m = 2\pi(m-1)/M$  denotes the angular location of the  $m$ th element.

a) *Beamforming:* The beamforming method computes the DOA by measuring the signal power at each possible angle of arrival and selecting the direction of maximum power as the estimate of the angle of arrival [8]. The drawback with the beamforming method is that the spatial resolution is determined by the number of antenna elements and inferior to the high-resolution subspace techniques. The power angular spectrum is given by:

$$P_{beamformer}(\theta, \varphi) = \mathbf{a}^H(\theta, \varphi) \hat{\mathbf{R}} \mathbf{a}(\theta, \varphi) \quad (5)$$

b) *MUSIC method:* MUSIC method is a subspace based algorithm, which offers high resolution in DoA estimation [8]. The basic idea is to search through the set of all possible steering vectors and find those that are orthogonal to the noise subspace. The power angular spectrum is given by:

$$P_{music}(\theta, \varphi) = \frac{1}{\mathbf{a}^H(\theta, \varphi) \hat{\mathbf{G}} \hat{\mathbf{G}}^H \mathbf{a}(\theta, \varphi)} \quad (6)$$

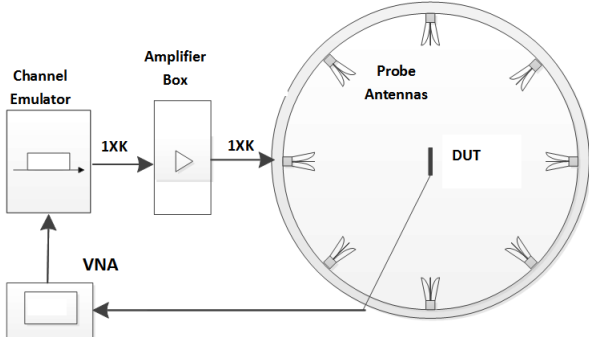


Figure 3. An illustration of the multi-probe based MIMO OTA setup.

where  $\hat{\mathbf{G}}$  is the noise subspace eigenvectors, which can be calculated from the auto-covariance matrix  $\hat{\mathbf{R}}$  [8]. Note that (6) is a “pseudo-spectrum”, as it only checks the orthogonality between steering vectors and the noise space, and hence power estimates in (6) are inconsistent.

3) *Signal power estimation*: Once the DoA estimates are obtained, we can estimate the average power of signals based on  $\hat{\mathbf{R}}$  and the DoA estimates. From (1) and (3), we have

$$\hat{\mathbf{R}} = E[\mathbf{x}[n]\mathbf{x}^H[n]] = \hat{\mathbf{A}}E[\mathbf{s}[n]\mathbf{s}^H[n]]\hat{\mathbf{A}}^H = \hat{\mathbf{A}}\hat{\mathbf{P}}\hat{\mathbf{A}}^H \quad (7)$$

where  $\hat{\mathbf{A}} = \{\mathbf{a}_m(\hat{\theta}_k, \hat{\varphi}_k)\} \in \mathbb{C}^{M \times K}$  is the steering matrix with  $\hat{\theta}_k$  and  $\hat{\varphi}_k$  the elevation and azimuth angle estimate for the  $k$ th signal, respectively.  $\hat{\mathbf{P}} \in \mathbb{R}^{K \times K}$  is a diagonal matrix with its  $k$ th element on the main diagonal  $p_k$  being the power estimate for the  $k$ th signal. This least-squared problem can be solved by the pseudo inverse:

$$\hat{\mathbf{P}} = (\hat{\mathbf{A}}^H \hat{\mathbf{A}})^{-1} \hat{\mathbf{A}}^H \hat{\mathbf{R}} (\hat{\mathbf{A}} \hat{\mathbf{A}}^H)^{-1} \hat{\mathbf{A}} \quad (8)$$

### III. SIMULATION AND MEASUREMENT RESULTS

#### A. Measurement setup

An illustration of a general multi-probe anechoic chamber setup is shown in Figure 3. The practical 3D probe configuration is shown in Figure 4. The measurement setup is summarized in Table I.  $\theta_i$  denotes the elevation angle for all the probes on  $i$ th elevation ring.  $\varphi_{ij}$  is the azimuth angle of the  $j$ th probe on the  $i$ th elevation ring. The measurement procedure is detailed in [1]. As a summary, the channel emulator pauses every 10 CIRs to satisfy Nyquist sampling criteria and the field is measured with the network analyzer. The dipole is then moved to next position, and the sweep of the same CIRs is repeated for the new position. This procedure is repeated until all the positions are covered. The virtual UCA is formed by repeating the same CIRs for all the positions.

#### B. Target models

Based on the preliminary setup, three target discrete PASs are selected, as detailed in Table II. Target model B approximates a single spatial cluster model, while target model C is selected to check the robustness of the virtual UCA for elevation angle estimation. Independent Rayleigh fading sequences with identical statistics are transmitted from the specified probes with known average power values.

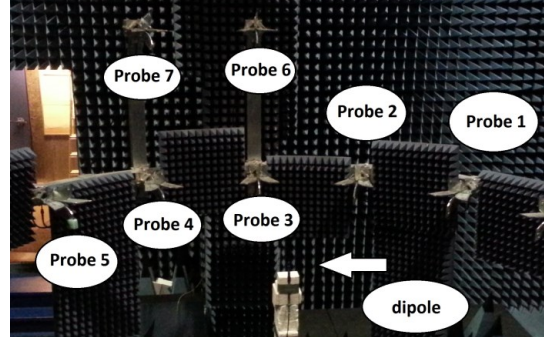


Figure 4. Probe configuration of the 3D practical multi-probe setup used in the measurements. The probe angular locations are detailed in Table I.

Table I  
SETUP AND SPECIFICATIONS FOR THE MEASUREMENTS

	Setup and specifications
Channel emulator	10000 channel impulse responses (CIRs) are created and stored. The CIRs are mapped to the OTA probes with known power weights
UCA	A Satimo calibration dipole at 2450MHz is rotated every $24^\circ$ with $r = 14$ cm to the center to form a virtual UCA.
Probe angular locations	The probes are organized on two elevation rings. 5 probes on the first ring with $\theta_1 = 90^\circ$ and $\varphi_{1j} = 135^\circ + (j-1) \cdot 22.5^\circ$ , $j \in [1, 5]$ . 2 probes on the second ring with $\theta_2 = 63.5^\circ$ and $\varphi_{2j} = 180^\circ + (j-1) \cdot 22.5^\circ$ , $j \in [1, 2]$ .

#### C. Results and discussions

Estimated DoAs based on simulations and measurements are compared for the three cases. Simulated DoAs match with the target in all cases as expected, see e.g. Figure 5 (left) for case A. The measured and simulated discrete PAS with beamforming technique match very well. With the MUSIC algorithm, deviation of azimuth DoA estimation (e.g.  $2.5^\circ$  as shown in Figure 5) is mainly caused by calibration error of dipole positions in measurement system and step accuracy of the turntable, since the estimated azimuth DoA match well with the target, with an offset around  $2^\circ$  for all the azimuth DoAs, as shown in Figure 6. As for the elevation DoA estimate, it is not robust in measurements as the virtual UCA's aperture is small in elevation, and hence the elevation DoA estimate is susceptible to the small noise in the system, as shown in Figure 5, 6, and 7 respectively.

Measured discrete PAS using MUSIC and beamforming algorithms for case B is shown in Figure 6. With the beamforming technique, only 3 probes with high power weights are detected due to the low spatial resolution and high sidelobes. The estimated discrete PAS using MUSIC and beamforming algorithms for the 3D probe configurations in measurements

Table II  
SETUP AND SPECIFICATIONS FOR THE MEASUREMENTS

Cases	Discrete PAS
A	Only probe 3 active
B	Probes 1, 2, 3, 4, 5 active with normalized average power shown in Figure 8 (left).
C	Probes 1, 5, 6 active with normalized average power shown in Figure 8 (right).

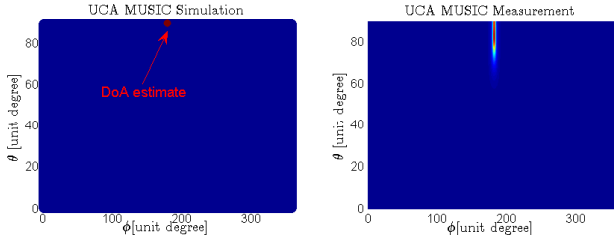


Figure 5. Simulated (left) and measured (right) discrete PAS using the MUSIC algorithm for case A. DOA estimate in the simulation is  $[180^\circ, 90^\circ]$  and DOA estimate in the measurement is  $[182.5^\circ, 84.5^\circ]$ .

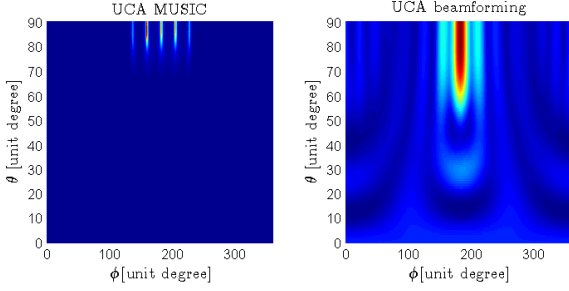


Figure 6. Measured discrete PAS using MUSIC and beamforming algorithms for case B. DOA estimate with MUSIC is  $[136.5^\circ, 88.5^\circ]$ ,  $[159.5^\circ, 85^\circ]$ ,  $[182.5^\circ, 87.5^\circ]$ ,  $[205^\circ, 87^\circ]$ ,  $[226.5^\circ, 88.5^\circ]$ , respectively.

are shown in Figure 7 and similar conclusions can be drawn.

Power estimates obtained in simulations using (8) match with the target in all cases, as expected. Power estimates in measurements are shown in Figure 8 for case B and case C, respectively. To demonstrate the impact of elevation angle estimation on the power estimate accuracy, power estimates obtained with the estimated azimuth angles  $\hat{\phi}$  and elevation angles  $\hat{\theta}$ , are compared with the case where power estimates are obtained with estimated azimuth angles  $\hat{\phi}$  and target elevation angles  $\theta$ . As shown in Figure 8, the power estimates are robust to elevation angle estimation inaccuracies. The power estimates using (8) generally match well with the target in case B. The power estimates with beamforming are consistent, though with worse accuracy due to the low spatial resolution and sidelobes impact. For case C, the power estimates present around 1dB deviation compared with the target. This might be introduced by the probe calibration inaccuracy.

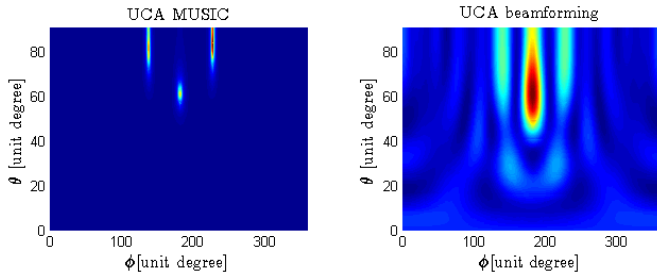


Figure 7. Measured discrete PAS using MUSIC and beamforming algorithms for case C. DOA estimate with MUSIC is  $[137.5^\circ, 83.5^\circ]$ ,  $[182.5^\circ, 63^\circ]$ ,  $[228.5^\circ, 86.5^\circ]$ , respectively.

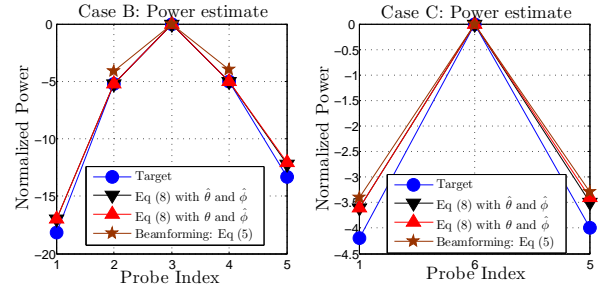


Figure 8. Signal power estimation results based on measurements for case B (left) and case C (right).

#### IV. CONCLUSION

We have introduced two techniques to estimate discrete power angular spectrum in the multi-probe based anechoic chamber setups, i.e. the beamforming and the MUSIC technique with power estimation. The beamforming technique provides consistent DoA and power estimates, which are prone to inaccuracy due to low spatial resolution and sidelobes. The MUSIC algorithm presents DoA estimates with high resolution. The power estimates based on DoA estimates match well with the target in the measurements. To improve accuracy and robustness in elevation DoA estimation, a virtual array with large aperture in elevation is suggested in measurements.

#### ACKNOWLEDGMENT

This work has been supported by the Danish National Advanced Technology Foundation via the 4GMCT project. The authors also appreciate the assistance from Intel Mobile Communications, Denmark in the measurements.

#### REFERENCES

- [1] "Verification of radiated multi-antenna reception performance of User Equipment," 3GPP, TR 37.977 V1.0.0, Sep. 2013.
- [2] D. Baum, J. Hansen, and J. Salo, "An interim channel model for beyond-3G systems: extending the 3GPP spatial channel model (SCM)," in *Proc. IEEE VTC-Spring*, May 2005.
- [3] W. Fan, X. de Lisbana, F. Sun, J. Nielsen, M. Knudsen, and G. Pedersen, "Emulating Spatial Characteristics of MIMO Channels for OTA Testing," *Antennas and Propagation, IEEE Transactions on*, vol. 61, no. 8, pp. 4306–4314, 2013.
- [4] P. Kyösti, T. Jämsä, and J. Nuutinen, "Channel modelling for multiprobe over-the-air MIMO testing," *International Journal of Antennas and Propagation*, 2012.
- [5] A. Khatun, H. Laitinen, V.-M. Kolmonen, and P. Vainikainen, "Dependence of Error Level on the Number of Probes in Over-the-Air Multiprobe Test Systems," *International Journal of Antennas and Propagation*, vol. 2012, 2012.
- [6] W. Fan, J. Nielsen, O. Franek, X. Carreno, J. Ashta, M. Knudsen, and G. Pedersen, "Antenna Pattern Impact on MIMO OTA Testing," *Antennas and Propagation, IEEE Transactions on*, vol. 61, no. 11, pp. 5714–5723, 2013.
- [7] W. Fan, F. Sun, P. Kyösti, J. Nielsen, X. Carreño, M. Knudsen, and G. Pedersen, "3D channel emulation in multi-probe setup," *Electronics Letters*, vol. 49, pp. 623–625(2), April 2013.
- [8] P. Stoica and R. L. Moses, *Spectral analysis of signals*. Pearson/Prentice Hall Upper Saddle River, NJ, 2005.